

## Lecture 11: Buckling of Plates and Sections

Most of steel or aluminum structures are made of tubes or welded plates. Airplanes, ships and cars are assembled from metal plates pined by welling riveting or spot welding. Plated structures may fail by yielding fracture or buckling. This lecture deals with a brief introduction to the analysis of plate buckling. A more complete treatment of this subject is presented in the 2.081 course of Plates and Shells, which is available on the Open Course. For additional reading, the following monographs are recommended:

1. Stephen P. Timoshenko and James M. Gere, Theory of Elastic Stability.
2. Don. O. Brush and Bo. O. Almroth, Buckling of Bars, Plates and Shells.

### 11.1 Governing Equations and Boundary Conditions

In the present notes the column buckling was extensively studied in Lecture 9. The governing equation for a geometrically perfect column is

$$EIw^{IV} + Nw'' = 0 \quad (11.1)$$

A step-by-step derivation of the plate buckling equation was presented in Lecture 7

$$D\nabla^4 w + \bar{N}_{\alpha\beta}w_{,\alpha\beta} = 0 \quad (11.2)$$

where  $\bar{N}_{\alpha\beta}$  is a set of constant, known parameters that must satisfy the governing equation of the pre-buckling state, given by Eqs. (7.10-7.12). The classical buckling analysis of plates is best explained on an example of a rectangular plate subjected to compressive loading in one direction, Fig. (11.1).

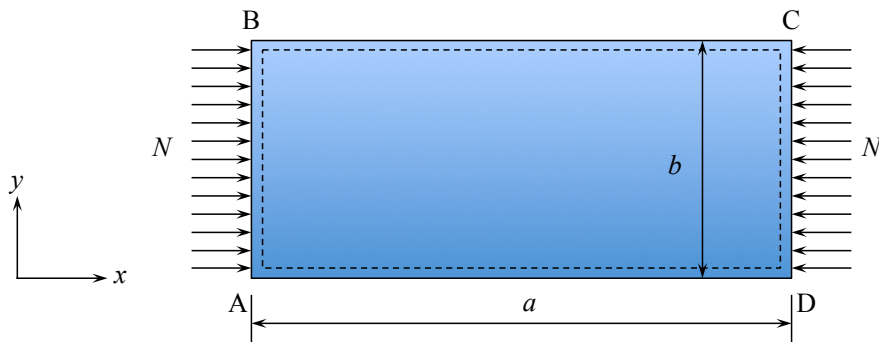


Figure 11.1: Geometry and loading of the classical plate buckling problem.

The plate is simply supported along all four edges. The edges AB and CD are called the loaded edges because in-plane loading  $N \left[ \frac{\text{N}}{\text{m}} \right]$  is applied to these edges. The other two

edges AD and BC are called the unloaded edges. The simply supported boundary conditions apply to vanishing of transverse deflections and the normal bending moments

$$w = 0 \quad \text{on ABCD} \quad (11.3a)$$

$$M_n = 0 \quad \text{on ABCD} \quad (11.3b)$$

Separate boundary condition must be formulated in the in-plane direction in the normal and tangential direction

$$(N_n - \bar{N}_n)\delta u_n = 0 \quad (11.4a)$$

$$(N_t - \bar{N}_t)\delta u_t = 0 \quad (11.4b)$$

In the case of the present rectangular plate Eqs. (11.3) reduce to

$$\left. \begin{array}{l} (N_{xx} - \bar{N}_{xx})\delta u_x = 0 \\ (N_{xy} - \bar{N}_{xy})\delta u_y = 0 \\ (N_{yy} - \bar{N}_{yy})\delta u_y = 0 \\ (N_{xy} - \bar{N}_{xy})\delta u_x = 0 \end{array} \right\} \begin{array}{l} \text{on AB and CD} \\ \text{on AD and BC} \end{array} \quad (11.5)$$

In the present problem the stress boundary conditions are applied and the tensor of external loading is

$$\bar{N}_{\alpha\beta} = \begin{vmatrix} \bar{N} & 0 \\ 0 & 0 \end{vmatrix}, \quad N_{\alpha\beta} = \begin{vmatrix} N & 0 \\ 0 & 0 \end{vmatrix} \quad (11.6)$$

With the above field of membrane forces the equilibrium equations are satisfied identically. From the constitutive equations

$$N_{xx} = C(\epsilon_{xx}^\circ + \nu\epsilon_{yy}^\circ) \quad (11.7a)$$

$$0 = C(\epsilon_{yy}^\circ + \nu\epsilon_{xx}^\circ) \quad (11.7b)$$

Therefore  $\epsilon_{yy}^\circ = -\nu\epsilon_{xx}^\circ$  and so  $N_{xx} = Eh\epsilon_{xx}^\circ$ . The displacement is calculated by solving two equations

$$\epsilon_{xx}^\circ = \frac{du_x}{dx} \quad (11.8a)$$

$$\epsilon_{yy}^\circ = \frac{du_y}{dy} \quad (11.8b)$$

With the origin of the coordinate system placed at the point A in Fig. (11.1), The solution is

$$u_x = u_o \left(1 - \frac{x}{a}\right), \quad u_y = \nu u_o \frac{y}{a}, \quad N = \frac{Eh}{a} u_o \quad (11.9)$$

Note that  $\bar{N}$  has been defined as positive in compression. Therefore the plate will be compressed in the x-direction and will expand laterally in the y-direction because of the effect of the Poisson ratio. In setting up the experiment or developing the FE model, the plate should be left free in the in-plane direction.

## 11.2 Buckling of a Simply Supported Plate

The expanded form of the governing equation corresponding to the assumed type of loading is

$$D \left[ \frac{\partial^4 w}{\partial x^4} + 2 \frac{\partial^4 w}{\partial x^2 \partial y^2} + \frac{\partial^4 w}{\partial y^4} \right] + \bar{N} \frac{d^2 w}{dx^2} = 0 \quad (11.10)$$

The solution of the above linear partial differential equation with constant coefficient is sought as a product of two harmonic functions

$$w(x, y) = \sin \frac{m\pi x}{a} \sin \frac{n\pi y}{b} \quad (11.11)$$

where  $m$  and  $n$  are number of half waves in the longitudinal and transverse directions, respectively. The function  $w(x, y)$  satisfies the boundary condition for displacement. The bending moment  $M_n$

$$M_n = M_{xx} = D[\kappa_{xx} + \nu \kappa_{yy}] = -D \left[ \left( \frac{m\pi}{a} \right)^2 + \nu \left( \frac{n\pi}{b} \right)^2 \right] \sin \frac{m\pi x}{a} \sin \frac{n\pi y}{b} \quad (11.12)$$

vanishes at  $x = 0$  and  $x = a$  edges. Also at  $y = 0$  and  $y = b$ ,  $M_n = M_{yy}$  is zero. Therefore the proposed function satisfy the simply supported boundary condition at all four edges. Substituting the function  $w(x, y)$  into the governing equation, one gets

$$\left\{ D \left[ \left( \frac{m\pi}{a} \right)^4 + 2 \left( \frac{m\pi}{a} \right)^2 \left( \frac{n\pi}{b} \right)^2 + \left( \frac{n\pi}{b} \right)^4 \right] - \bar{N} \left( \frac{m\pi}{a} \right)^2 \right\} \sin \frac{m\pi x}{a} \sin \frac{n\pi y}{b} = 0 \quad (11.13)$$

The differential equation is satisfied for all values of  $(x, y)$  if the coefficients satisfy

$$\bar{N} = D \left( \frac{\pi a}{m} \right)^2 \left[ \left( \frac{m}{a} \right)^2 + \left( \frac{n}{b} \right)^2 \right]^2 \quad (11.14)$$

It is seen that the smallest value of  $\bar{N}$  for all values of  $a$ ,  $b$  and  $m$  is obtained if  $n = 1$ . This means that only one half wave will be formed in the direction perpendicular to the load application. Then, Eq. (11.12) can be put into a simple form

$$\bar{N}_c = k_c \frac{\pi^2 D}{b^2} \quad (11.15)$$

where the buckling coefficient  $k_c$  is a function of both the plate aspect ratio  $a/b$  and the wavelength parameter

$$k_c = \left( \frac{mb}{a} + \frac{a}{mb} \right)^2 \quad (11.16)$$

The parameter  $m$  is an integer and determines how many half waves will fit into the length of the plate. The aspect ratio  $a/b$  is known, but the wavelength parameter is still unknown. Its value must be found by inspection, i.e., by plotting the buckling coefficient as a function of  $a/b$  for subsequent values of the parameter  $m$ . This is shown in Fig. (11.2).

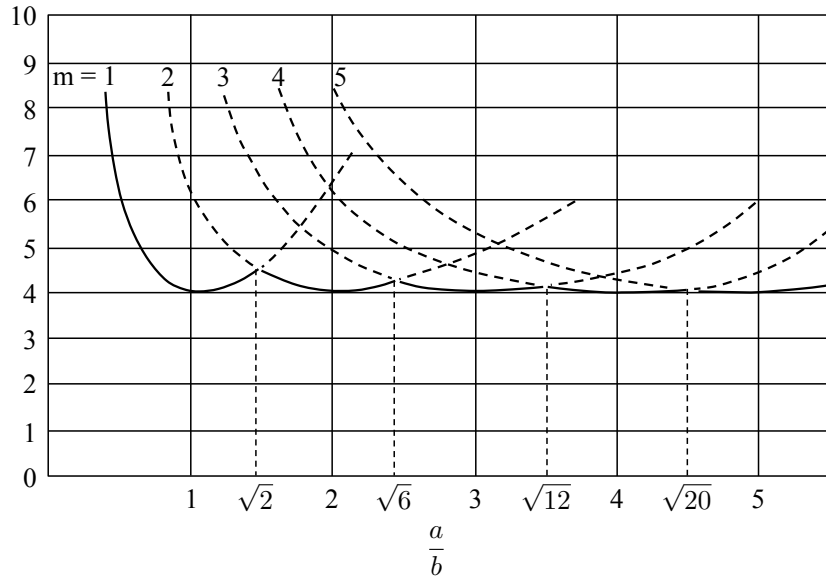


Figure 11.2: Plot of the buckling coefficient for a simply supported plate as a function of the plate aspect ratio  $a/b$  and different wave numbers.

For example, the buckling coefficient corresponding to the first five buckling modes corresponding to  $\frac{a}{b} = 2$  are

Table 11.1:

$m$	1	2	3	4	5
$k_c$	6.2	4	4.7	6.2	8.4

The lowest buckling load  $k_c = 4$  occurs when there are two half waves along the length of the plate,  $m = 2$ . The line separating the safe, shaded area in Fig. (11.2) and the unsafe while area defines uniquely the buckling coefficient for all combination of  $a/b$  and  $m$ .

Consider now a long plate,  $a \gg b$  for which the parameter  $m$  can be treated as a continuous variable. In this case there is an analytical minimum of the buckling coefficient

$$\frac{dk_c}{dm} = 0 \quad \rightarrow \quad a = mb \quad (11.17)$$

The above result means that the plate divides itself into an integer number of squares with alternating convex and concave dimples.

What happens when the rectangular plate shown in Fig. (11.1) is restricted from lateral expansion

$$u_y(y = 0) = u_y(y = b) = 0 \quad (11.18)$$

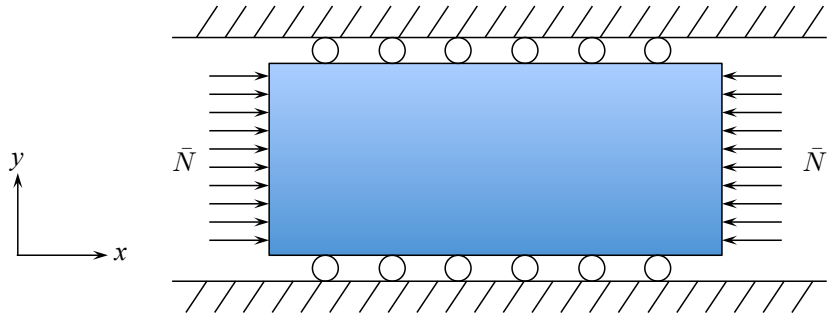


Figure 11.3: Constrained compression of the plate.

With no strain in the  $y$ -direction,  $\epsilon_{yy} = 0$ , the constitutive equations (11.6) reduces to

$$N_{xx} = C\epsilon_{xx}^\circ \quad (11.19a)$$

$$N_{yy} = C\nu\epsilon_{xx}^\circ \quad (11.19b)$$

This means that a reaction force  $N_{yy} = \nu N_{xx}$  develops in the transverse direction. The buckled shape of the plate is the same and the solution, Eq. (??) still holds but the new expression for the buckling coefficient is

$$k_c = \frac{\left[ \left( \frac{mb}{a} \right)^2 + n^2 \right]^2}{\left( \frac{mb}{a} \right)^2 + \nu n^2} \quad (11.20)$$

The least value of the buckling coefficient can be found by inspection. Taking again as an example  $a/b = 2$ , the values of the buckling coefficient corresponding to the nine first buckling modes are

Table 11.2:

$n \backslash m$	1	2	3
1	10.7	3	4.09
2	3.8	10.7	10.9
3	26	25	24.1

The lowest value of the buckling coefficient  $k_c = 3$  corresponds to two half-waves in the loading direction and one half wave in the transverse direction. It is seen that restricting the in-plane deformation does not change the buckling mode but reduces the buckling load by a factor of  $3/4$ . The reaction compressive force makes the plate to buckle more easily. This example underscores the importance of properly defining the boundary conditions not only in the out-of-plane direction but also in the in-plane directions.

### 11.3 Effect of Boundary Conditions

The unloaded edges of rectangular plates can be either simply supported (ss), clamped (c) or free. (The sliding boundary conditions will convert the eigenvalue problem into the equilibrium problem and therefore are not considered in the buckling analysis of plates). The loaded edges could be either simply supported or clamped. This gives rise to ten different combination. The buckling coefficient is plotted against the plate aspect ratio  $a/b$  for all these combinations in Fig. (11.4). It is seen that the lowest buckling coefficient with  $m = 1$  corresponds to a simply supported plate on three edges and free on the fourth edge.

An approximate analytical solution for the case “E” was derived by Timoshenko and Gere in the form

$$k_c = 0.456 + \left(\frac{b}{a}\right)^2 \quad (11.21)$$

For example  $k_c = 0.706$  for  $a/b = 2$ , which is very close to the value that could be read off from Fig. (11.4). An angle element, shown in Fig. (11.5) is composed of two plates that are simply supported along the common edge and free on the either edges. Both plates rotate by the same amount at the common edges so that no edge restraining moment is developed. This corresponds to a simply supported boundary conditions.

In a similar way it can be proved that the prismatic square column consists of four simply supported long rectangular plates. Upon compression, the buckling pattern has a form shown in Fig. (11.6). Again, there are no relative rotations at the intersection line of any of the neighboring plates ensuring the simply supported boundary condition along four edges.

Another very practical case is shear loading. For example “I” beams with a relatively high web or girders may fail by shear buckling, Fig. (11.7), in the compressive side when subjected to bending.

The solution to the shear buckling is much more complicated than in the previous cases of compressive buckling. The general form of the solution is still given by Eq. (??) but there is no simple closed form solution for the buckling coefficient. An approximate solution for  $k_c$ , derived by Timoshenko and Gere has the form

$$k_c = 5.35 + 4 \left(\frac{b}{a}\right)^2 \quad (11.22)$$

For a square plate the buckling coefficient is 9.35 while for an infinitely long plate,  $a \gg b$  it reduces to 5.35. Loading the plate in the double shear experiment for beyond the elastic buckling load produces a set of regular skewed dimples seen in Fig. (11.8).

### 11.4 Buckling of Sections

Cold-form or welded profiles are encountered in almost every aspect of the engineering practice. Typical cross-sectional geometries of prismatic members are shown in Fig. (11.9).

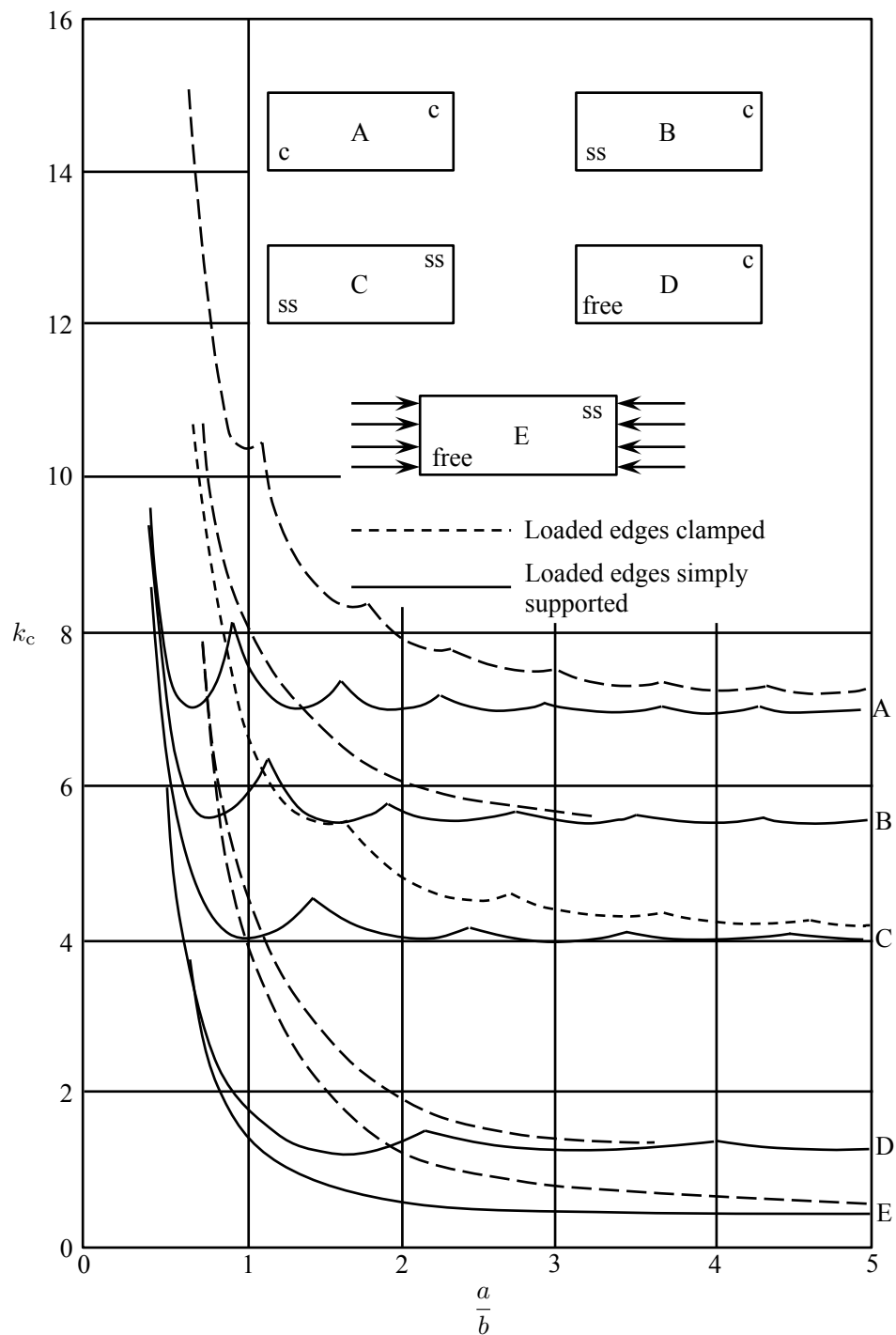


Figure 11.4: Effect of boundary conditions on the buckling coefficient of rectangular plates subjected to in-plane boundary conditions.

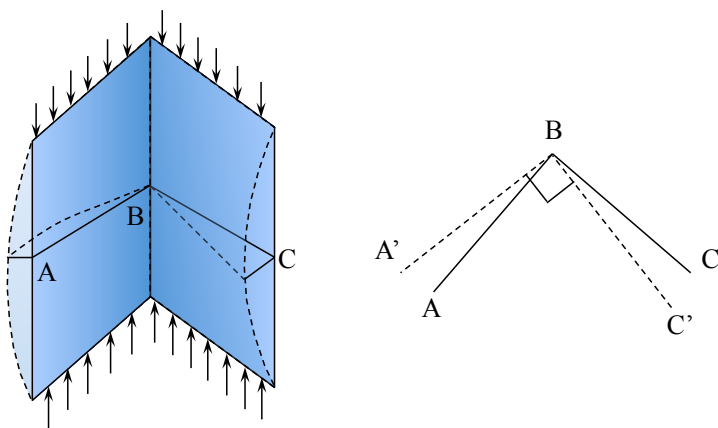


Figure 11.5: Buckling mode of an angle element.

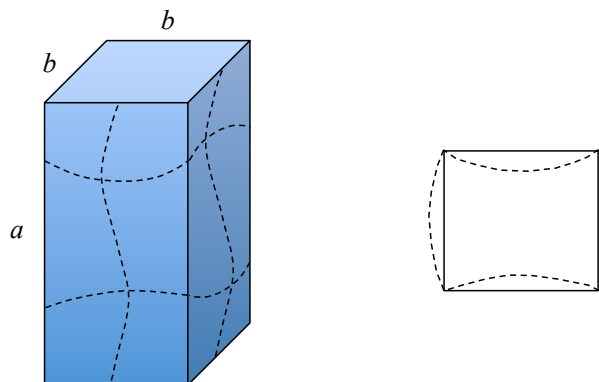


Figure 11.6: The buckling mode of a prismatic square column.

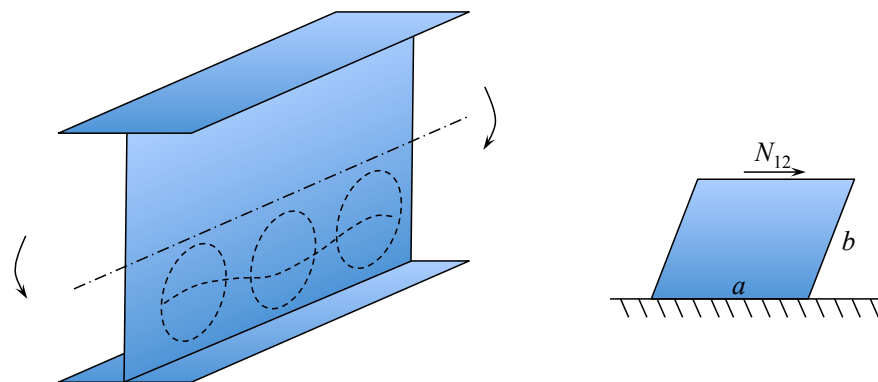


Figure 11.7: Buckling due to shear or bending.

Except of symmetric angle, "T", cruciform and square box profile where buckling strength of the entire section is a sum of buckling loads of contributing plates, the analysis of other shape requires consideration of restraining bending moments and continuity con-



Figure 11.8: A photograph of shear buckling of a plate representing the damage pattern on the ship's hull inflicted upon grounding.

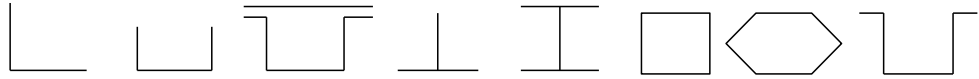


Figure 11.9: Some typical open and closed cross-sectional shape of prismatic members.

ditions along the common edges. The easiest way to illustrate the problem is to consider a rectangular section prismatic column, Fig. (11.10). According to Eq. (??) the buckling load is inversely proportional to the width of the plate. The two opposite wider plates would like to buckle first, but the shorter sides are not ready to buckle with  $k = 4$ . They provide clamped boundary condition for the wider flanges for which  $k \cong 7$ . There must be a transfer of information between the adjacent plates so that they will buckle “in sympathy” to one another with a different  $k_c$ .

The numerically obtained function  $k_1(b_2/b_1)$  is shown in Fig. (11.10) by a solid line. The buckling coefficient is uniquely related to  $k_1$  through the pre-buckling analysis. Before buckling the strains and compressive stresses in the adjacent plates are the same

$$\sigma_1 = \frac{N_1}{h_1} = \sigma_2 \frac{N_2}{h_2} \quad (11.23)$$

where

$$N_1 = k_1 \frac{\pi^2 D_1}{b_1^2}, \quad N_2 = k_2 \frac{\pi^2 D_2}{b_2^2} \quad (11.24)$$

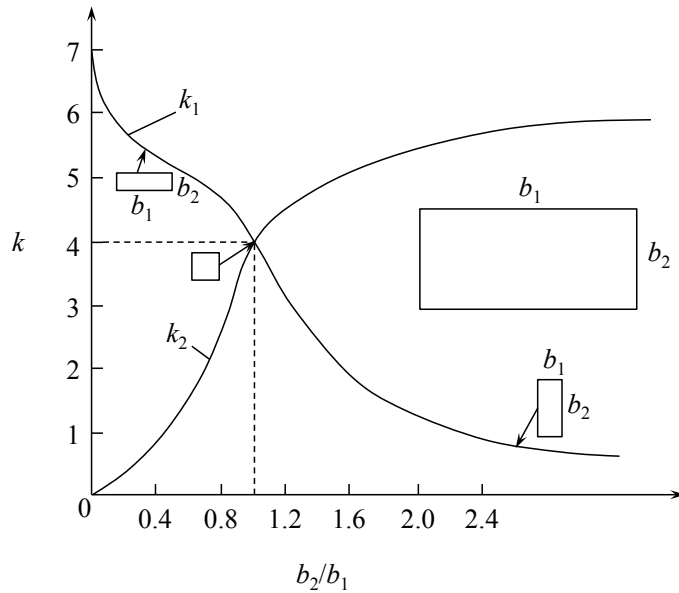


Figure 11.10: Buckling coefficients of a rectangular plate as a function of  $b_2/b_1$ .

From the above equation it follows that

$$k_2 = k_1 \left( \frac{b_2}{b_1} \right)^2 \quad (11.25)$$

$k_1$  is shown in Fig. (11.10) (solid line). The buckling coefficient  $k_2$  calculated from Eq. (??) is shown on the same figure by the dashed line. With the above result one can prove that for a given weight (cross-section area) the square column will have the largest buckling resistance for all rectangular shapes.

For more complex cross-sectional shape the buckling coefficient can be presented in a graphical form, as shown in Fig. (11.11). Knowing the buckling coefficient  $k_1$  for a flange with the width  $b_1$  and thickness  $h_1$ , the buckling coefficients of all other flanges is then calculated from:

$$k_i = k_1 \left( \frac{h_i b_1}{h_1 b_i} \right) \quad (11.26)$$

In most cases nothing dramatic happens at the point of buckling. The purely compressive state switches into a combined bending/compression but the plate continues to carry additional load with a reduced stiffness. The post-buckling and ultimate load response is discussed in the next section of this lecture.

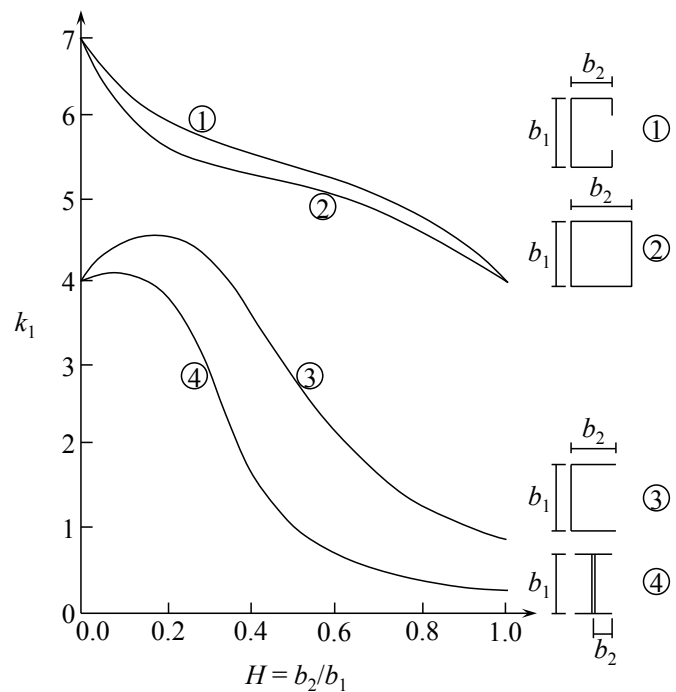


Figure 11.11: Buckling coefficients for four types of sections.

## ADVANCED TOPIC

### 11.5 Post-buckling Response of Plates

Let's assumed that the plate is subjected to a monotonically increasing axial compression  $u_o$ , Fig. (11.12).

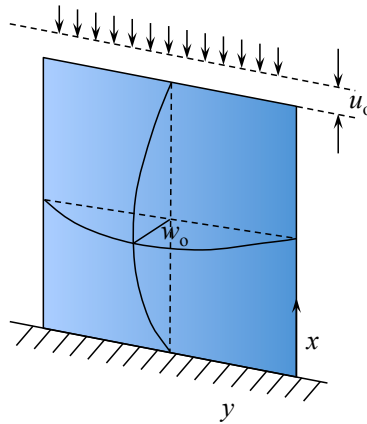


Figure 11.12: Two degree-of-freedom model of the buckled plate.

Initially the plate is straight and in the pre-buckling state there is uniaxial compression and bi-axial deformation. This stage was analyzed in section 7.1. there was no out-of-plane displacement  $w_o$ . The bifurcation point was tested by imposing an arbitrary small field of out-of-plane displacement. Now, some of the compression energy is relieved, but the bending energy appears so that the total potential energy of the system remains the same.

The corresponding value of the load (buckling load) under which this happens was derived in Section 7.2. What happens to the plate after buckling has occurred is the subject of the present section. The deformation of the plate is assumed to be a superposition of the in-plane compression. The form of the in-plane displacement is similar as in the pre-buckling solution, Eq. (??), but now one more term should be added to the expression for  $u_y$  in order to satisfy zero traction at the unloaded edges.

$$u_x = u_o \left(1 - \frac{x}{a}\right) \quad (11.27a)$$

$$u_y = \nu u_o \frac{y}{a} + f(x) \quad (11.27b)$$

The field of out-of-plane deformation is taken identical as in the buckling solution

$$w = w_o \sin \frac{\pi x}{a} \sin \frac{\pi y}{b} \quad (11.28)$$

which satisfies the simply supported boundary conditions at all four edges. Here it is assumed that the plate is either infinitely long or is square so that  $a = b$ .

The total potential energy of the system is

$$\Pi = U_b + U_m - PU_o \quad (11.29)$$

where  $P = bN$  and expression for the bending and membrane energies are given by Eqs. (4.73) and (4.86), respectively. The curvature tensor is defined by

$$\kappa_{\alpha\beta} = -w_{,\alpha\beta} \quad (11.30)$$

and for the assumed shape  $w(x, y)$  has three components

$$\kappa_{\alpha\beta} = w_o \left(\frac{\pi}{a}\right)^2 \begin{vmatrix} \sin \frac{\pi x}{a} \sin \frac{\pi y}{a} & -\cos \frac{\pi x}{a} \cos \frac{\pi y}{a} \\ -\cos \frac{\pi x}{a} \sin \frac{\pi y}{a} & \sin \frac{\pi x}{a} \sin \frac{\pi y}{a} \end{vmatrix} \quad (11.31)$$

The membrane strain results from the gradient of in-plane displacement vector and the moderately large rotation of plate elements

$$\epsilon_{\alpha\beta} = \frac{1}{2}(u_{\alpha,\beta} + u_{\beta,\alpha}) + \frac{1}{2}w_{,\alpha}w_{,\beta} \quad (11.32)$$

The components of the in-plane strain tensors are

$$\left. \begin{aligned} \epsilon_{xx} &= -\frac{u_o}{a} + \frac{w_o^2}{2} \left(\frac{\pi}{a}\right)^2 \cos^2 \frac{\pi x}{a} \sin^2 \frac{\pi y}{a} \\ \epsilon_{yy} &= \nu \frac{u_o}{a} + f'(x) + \frac{w_o^2}{2} \left(\frac{\pi}{a}\right)^2 \sin^2 \frac{\pi x}{a} \cos^2 \frac{\pi y}{a} \end{aligned} \right\} \quad (11.33)$$

$$\epsilon_{xy} = \frac{w_o^2}{2} \left(\frac{\pi}{a}\right)^2 \cos^2 \frac{\pi x}{a} \cos^2 \frac{\pi y}{a} \quad (11.34)$$

It is seen that the form of the axial strain  $\epsilon_{xx}$  provides coupling between the in-plane amplitude  $u_o$  and the out-of-plane amplitude  $w_o$ .

The general expression for the bending energy of the plate, Eq. (4.73) is

$$U_b = \frac{D}{2} \int_0^a \int_0^a \{(\kappa_{xx} + \kappa_{yy})^2 - 2(1-\nu)\kappa_G\} dx dy \quad (11.35)$$

where  $\kappa_G = \kappa_{xx}\kappa_{yy} - \kappa_{xy}^2$  is the Gaussian curvature. It can be easily shown that the Gaussian curvature integrated over the surface of the plate is zero. Therefore, the second term in the integrand of Eq. (11.21) vanishes. Finally, the total bending energy of the plate is calculated to be

$$U_b = \frac{1}{2} D w_o^2 \frac{\pi^4}{a^2} \quad (11.36)$$

Before proceeding to calculate the membrane strain energy, the unknown function  $f(x)$  in Eq. (??) should be determined from the boundary condition  $N_{yy}(y = a \text{ and } y = 0) = 0$ . The plane stress elasticity law is

$$N_{xx} = C(\epsilon_{xx} + \nu\epsilon_{yy}) \quad (11.37a)$$

$$N_{yy} = C(\epsilon_{yy} + \nu\epsilon_{xx}) \quad (11.37b)$$

$$N_{xy} = (1-\nu)C\epsilon_{xy} \quad (11.37c)$$

From Eq. (11.19), the in-plane membrane force in the  $y$ -direction is

$$N_{yy} = C \left[ \nu \frac{u_o}{a} + \frac{1}{2} w_o^2 \left( \frac{\pi}{a} \right)^2 \sin^2 \frac{\pi x}{a} \cos^2 \frac{\pi y}{a} + f' - \nu \frac{u_o}{a} + \frac{\nu}{2} w_o^2 \left( \frac{\pi}{a} \right)^2 \cos^2 \frac{\pi x}{a} \sin^2 \frac{\pi y}{a} \right] \quad (11.38)$$

The membrane force changes from point to point and at the unloaded edges  $y = 0$  and  $y = a$  is

$$N_{yy}(0, a) = C \left[ \frac{1}{2} w_o^2 \left( \frac{\pi}{a} \right)^2 \sin^2 \frac{\pi x}{a} + f' \right] \quad (11.39)$$

Now, the total membrane energy of the plate can be calculated. After lengthy algebra, the final expression is

$$U_m = \frac{C}{2} \left[ (1 - \nu^2) u_o^2 - 2(1 - \nu^2) \frac{\pi^2}{8} \frac{u_o}{a} w_o^2 + (3 - 2\nu) \frac{\pi^4}{64} \frac{w_o^4}{a^2} \right] \quad (11.40)$$

The total potential energy of the system is

$$\Pi(u_o, w_o) = U_b + U_m - P u_o \quad (11.41)$$

The equilibrium of the system requires that the first variation of the total potential energy vanishes  $\delta\Pi(u_o, w_o) = 0$ . This leads to two equations

$$\frac{\partial\Pi}{\partial u_o} = 0 \quad \rightarrow \quad P = (1 - \nu^2) C \left[ u_o - \frac{\pi^2}{8} \frac{w_o^2}{a} \right] \quad (11.42)$$

$$\frac{\partial\Pi}{\partial w_o} = 0 \quad \rightarrow \quad 64 \left( \frac{\pi}{a} \right)^2 w_o \left[ \frac{4\pi^2 D}{C} - (1 - \nu^2) a u_o + (3 - 2\nu) \frac{\pi^2}{8} w_o^2 \right] = 0 \quad (11.43)$$

There are two solutions of the above system. The pre-buckling solution is recovered by setting  $w_o = 0$ . Then from Eq. (??)

$$P = (1 - \nu^2) C u_o = (1 - \nu^2) \frac{Eh}{1 - \nu^2} u_o = Ehu_o \quad (11.44)$$

and Eq. (??) is satisfied identically. The solution (??) is exact and is equal to the one derived in Section 11.1 of Lecture 11. In the post-buckling range  $w_o > 0$  and Eq. (??) provides a unique relation between the in-plane and out-of-plane amplitude of the assumed displacement field

$$\frac{\pi^2}{8} \left( \frac{w_o}{a} \right)^2 = \frac{1 - \nu^2}{3 - 2\nu} \frac{u_o}{a} - \frac{4D\pi^2}{C(3 - 2\nu)a^2} \quad (11.45)$$

The plot of the function  $w_o = w_o(u_o)$  is shown in Fig. (11.13).

The critical displacement  $(u_o)_c$  to buckle, corresponding to the point of buckling, is obtained from Eq. (??) by setting  $w_o = 0$

$$(u_o)_c = \frac{4\pi^2 D}{a} \frac{1}{C(1 - \nu^2)} \quad (11.46)$$

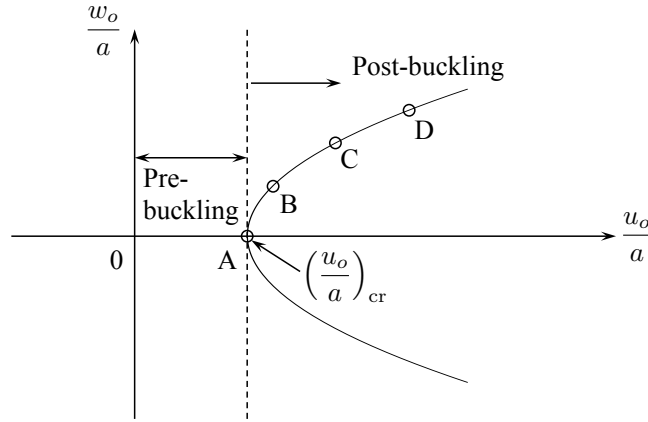


Figure 11.13: The out-of-plane displacement amplitude.

Eliminating  $w_o$  between Eqs. (??) and (??) gives a linear post-buckling solution

$$P = \frac{13}{25}(1 - \nu^2)Cu_o + \frac{1 - \nu^2}{3 - 2\nu} \frac{4\pi^2 D}{a} \quad (11.47)$$

The post-buckling stiffness  $K_{\text{post}} = \frac{dD}{du_o}$  is

$$K_{\text{post}} = \frac{13}{25}(1 - \nu^2)C = 0.52K_{\text{pre}} \quad (11.48)$$

where  $K_{\text{pre}}$  is the pre-buckling stiffness. For all practical purposes it can be assumed that the plate is losing half of its stiffness after buckling but is able to carry additional loads. Based on the above analysis, the load-displacement relation of an elastic plate is depicted in Fig. (11.14).

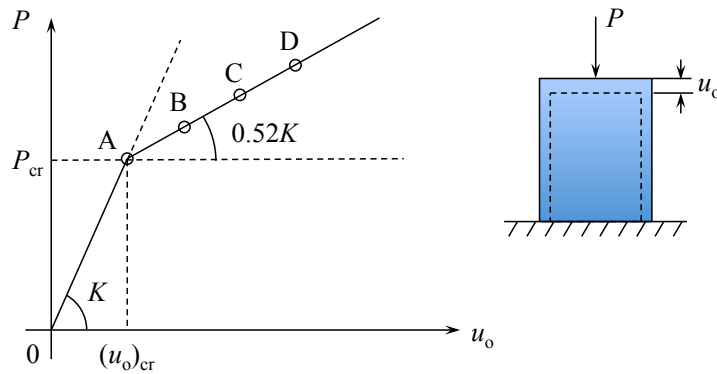


Figure 11.14: Pre and post-buckling response of a plate.

Substituting the expression for  $(u_o)_c$  into Eq. (11.44), the predicted buckling load is

$$P_c = \frac{4\pi^2 D}{a} \quad (11.49)$$

which is the exact solution of the problem.

## **END OF ADVANCED TOPIC**

## 11.6 Ultimate Strength of Plates

In the previous section we have shown that after buckling the plate continues to take additional load but with half of its pre-buckling stiffness. In order to understand what happens next, let's examine the distribution of in-plane compressive stresses  $\sigma_{xx}$  at  $x = a$ . From Eqs. (11.19) and (??) the components  $\sigma_{xx}$  is

$$\sigma_{xx}(y) = \frac{N_{xx}}{h} = \frac{E}{1 - \nu^2} \left[ -(1 - \nu^2) \frac{u_o}{a} + \frac{\pi^2}{2} \left( \frac{w_o}{a} \right)^2 \sin^2 \frac{\pi y}{a} \right] \quad (11.50)$$

The first term represents negative, compressive stress, uniform along the width of the plate. The second term describes the relieving tensile stress produced by finite rotation. The relation between  $w_o$  and  $u_o$  is given by Eq. (??) and is depicted in Fig. (11.13). A plot of the function  $\sigma_{xx}(y)$  for several values of the time-like parameter  $u_o$  is shown in Fig. (11.15). Note that the curves labeled A, B, C and D corresponds to the respective points in Figs. (11.13) and (11.14).

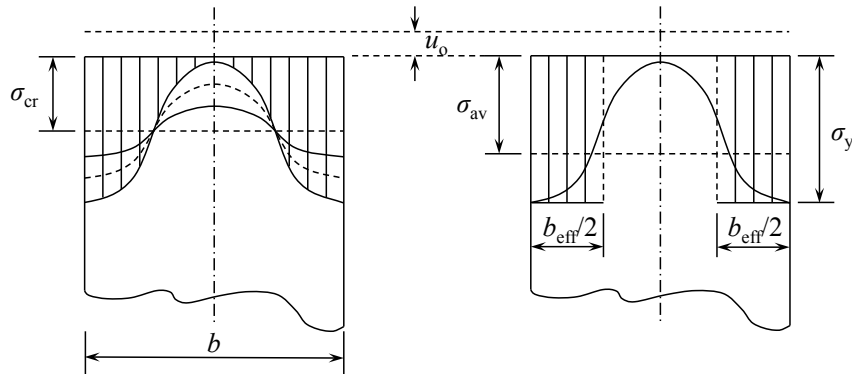


Figure 11.15: Re-distribution of compressive stresses along the loaded edge and simple approximation by von Karman.

With increasing plate compression there is a re-distribution of stresses along the loaded edge  $x = 0$  and  $x = a$ . The stress at the unloaded edge  $y = 0$  and  $y = a$  keeps increasing while the stress at the plate symmetry plane  $y = \frac{a}{2}$  diminishes to zero.

It was the German scientist and engineer, Theodore von Karman who in 1932 made use of the observation presented in Fig. (11.15). He assumed that the central, unloaded portion of the plate carries zero stress while the edge zone, each of the width  $b_{\text{eff}}/2$  reaches the yield stress at the point of ultimate load. As a starting point, von Karman used the expression for the critical buckling load  $N_c$  and looked at the relation between the stress at the loaded edge  $\sigma_e$  and the plate width  $b$

$$\sigma_e = \frac{N_e}{h} = \frac{N_c}{h} = \frac{4\pi^2 D}{hb^2} = \frac{4\pi^2 Eh^2}{12(1 - \nu^2)b^2} = 1.9^2 E \left( \frac{h}{b} \right)^2 \quad (11.51)$$

Normally  $b$  is the input parameter and the stress  $\sigma_e$  is an unknown quantity. The ingenuity of von Karman was that he inverted what is known and unknown in Eq. (??). He asked

what should be the width of the plate  $b_{\text{eff}}$  so that the edge stress reaches the yield stress. Thus

$$\sigma_y = 1.9^2 E \left( \frac{h}{b_{\text{eff}}} \right)^2 \quad (11.52)$$

Solving the above equation for  $b_{\text{eff}}$

$$b_{\text{eff}} = 1.9 h \sqrt{\frac{E}{\sigma_y}} \quad (11.53)$$

Taking for example  $E = 200000$  MPa,  $\sigma_y = 320$  MPa, the effective width becomes

$$b_{\text{eff}} = 1.9 h \sqrt{625} = 47.5 h \quad (11.54)$$

The effective width depends on the Young's modulus and yield stress is proportional to the plate thickness. Approximately 40-50 thicknesses of the plate near the edges carries the load, the remaining central part is not effective. The total load on the plate can be expressed in two ways

$$P_{\text{ult}} = b_{\text{eff}} \cdot \sigma_y = b \cdot \sigma_{\text{av}} \quad (11.55)$$

where  $\sigma_{\text{av}} = \sigma_{\text{ult}}$  is the average stress on the loaded edge at the point of ultimate strength,

$$\frac{\sigma_{\text{av}}}{\sigma_{\text{ult}}} = \frac{b_{\text{eff}}}{b} = 1.9 \frac{h}{b} \sqrt{\frac{E}{\sigma_y}} \quad (11.56)$$

The group of parameters

$$\beta = \frac{b}{h} \sqrt{\frac{\sigma_y}{E}} \quad (11.57)$$

is referred to as the slenderness ratio of the plate. Note that this is a different concept than the slenderness ratio of the column  $l/\rho$ . Using the parameter  $\beta$ , the ultimate strength of the plate normalized by the yield stress is

$$\frac{\sigma_{\text{ult}}}{\sigma_y} = \frac{1.9}{\beta} \quad (11.58)$$

Recall that the normalized buckling stress of the elastic plate is

$$\frac{\sigma_{\text{cr}}}{\sigma_y} = \left( \frac{1.9}{\beta} \right)^2 \quad (11.59)$$

Plots of both functions are shown in Fig. (11.16).

From this figure one can identify the critical slenderness ratio

$$\beta_{\text{cr}} = 1.9 \quad (11.60)$$

when both the ultimate load and the critical buckling load reach yield. From Eq. (??) one can see that at  $\beta = \beta_{\text{cr}}$ , the effective width is equal to the plate width,  $b_{\text{eff}} = b$ .

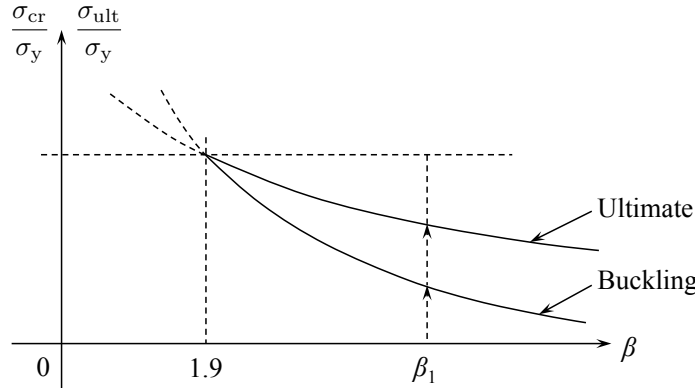


Figure 11.16: Dependence of the buckling stress and ultimate stress on the slenderness ratio.

Eliminating the parameter  $\beta$  between Eqs. (??) and (??), the ultimate stress is seen to be the geometrical average between the yield stress and critical buckling stress

$$\sigma_{\text{ult}} = \sqrt{\sigma_{\text{cr}} \cdot \sigma_y} \quad (11.61)$$

For example, continuous loading of a plate with the slenderness ratio  $\beta_1$  will first encounter the buckling curve and then the ultimate strength curve, as illustrated in Fig. (11.16). The foregoing analysis was valid for plates simply supported along all four edges, for which the buckling coefficient is  $k_c = 4$ . For other type of support Eq. (??) is still valid with the coefficient 1.9 replaced by  $1.9 \frac{k_c}{4}$ .

Much effort has been devoted in the past to validate experimentally the prediction of the von Karman effective width theory. It was found that a small correction to Eq. (??) provides good fit of most of the test data

$$\frac{\sigma_{\text{ult}}}{\sigma_y} = \frac{b_{\text{eff}}}{b} = \frac{1.9}{\beta} - \frac{0.9}{\beta^2} \quad (11.62)$$

For example, for a relatively short (stocky plate)  $\beta = 2\beta_{\text{cr}} = 3.8$ , the original formula over predicts by 15% than the more exact empirical equation (??). For slender plates, the difference is small. The latter has been the basis for the design of thin-walled compressive elements in most domestic and international standards such as AISI, Aluminum Association and AISC.

## 11.7 Effect of Initial Imperfection

Plates may be geometrically imperfect due to the manufacturing process, welding distortion or mishandling during transportation. The shape of the imperfect plate can be measured as is defined by the function  $\bar{w}(x, y)$ . In general the initial out-of-plane shape can be expanded in a Fourier series. The first fundamental mode grows more rapidly. Therefore it is sufficient

to consider that imperfections are distributed in the first mode

$$\bar{w}(x, y) = \bar{w}_o \sin \frac{\pi x}{a} \sin \frac{\pi y}{a} \quad (11.63)$$

With the initial imperfection the definition of the curvatures and membrane strains must be modified

$$\kappa_{\alpha\beta} = -(w - \bar{w})_{,\alpha\beta} \quad (11.64)$$

$$\epsilon_{\alpha\beta} = \frac{1}{2}(u_{\alpha,\beta} + u_{\beta,\alpha}) + \frac{1}{2}w_{,\alpha}w_{,\beta} - \frac{1}{2}\bar{w}_{,\alpha}\bar{w}_{,\beta} \quad (11.65)$$

which reduce to Eqs. (11.16) and (11.5), respectively, when  $\bar{w}(x, y) = 0$ . The derivation presented in Section 11.5 is still valid and the expression for the total potential energy is the same, except all terms involving  $w_o$  should now be replaced by  $(w_o - \bar{w}_o)$ . The structural imperfections are usually small and comparable to the thickness of the plate. A plot of the load-displacement curve for the geometrically perfect plate and the plate with two magnitudes of initial imperfections is shown in Fig. (11.17). The load has been normalized with the critical buckling load and displacements by the critical buckling displacement.

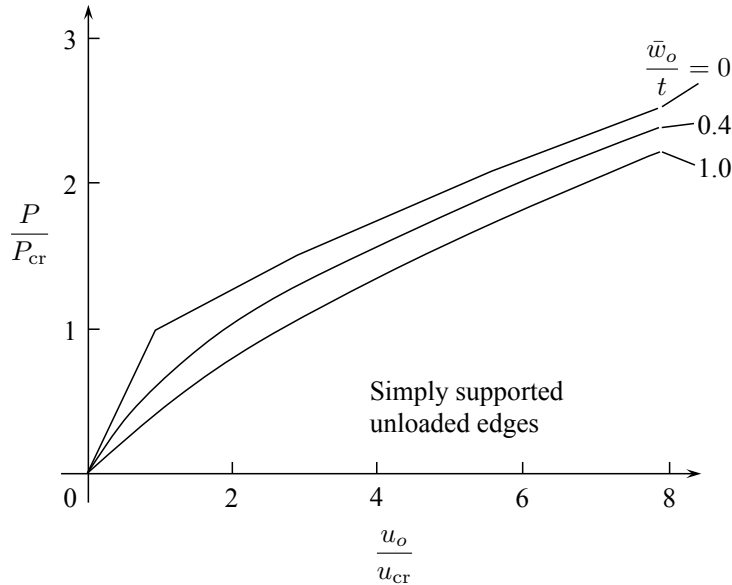


Figure 11.17: Load-displacement curves for imperfect simply supported plates.

MIT OpenCourseWare  
<http://ocw.mit.edu>

2.080J / 1.573J Structural Mechanics  
Fall 2013

For information about citing these materials or our Terms of Use, visit: <http://ocw.mit.edu/terms>.